REVISION 2

Kumdykolite from the ultrahigh-pressure granulite of the Bohemian Massif

Jana Kotková [1,2], Radek Škoda [2] and Vladimír Machovič [3]

[1]Czech Geological Survey, Klárov 3, 118 21 Prague 1, Czech Republic

[2]Dept. of Geological Sciences, Masaryk University, Kotlářská 2, 611 37 Brno, Czech Republic

[3] Institute of Chemical Technology Prague, Technická 5, 166 28 Prague 6, Czech Republic

Abstract

We report the first occurrence of kumdykolite, a high-temperature analog of albite, in the European Variscan belt. It was discovered in an ultrahigh-pressure, diamond-bearing quartzofeldspathic granulite from the northern Bohemian Massif. It is associated with phlogopite and quartz in a multiphase solid inclusion within garnet, considered to represent a trapped fluid or melt phase. Micro-Raman analysis and mapping along with BSE revealed the presence of a sub-equant, elongated grain of kumdykolite reaching 20 μm in length. WDX analysis has shown that kumdykolite contains 2 wt. % CaO, probably indicating significant miscibility with the Ca-endmember svyatoslavite. Similar to the case of microdiamond inclusions, the kumdykolite-bearing multiphase inclusion is located in the Ca- and Mg-rich central part of the garnet and thus must have been trapped at $P > 4$ GPa. The inclusion minerals, however, crystallized upon decompression and cooling during the exhumation. Kumdykolite preservation thus provides independent evidence for high temperature of the original trapped fluid, or melt, crystallization, and rapid cooling of the rocks. Our results imply that kumdykolite and other feldspar modifications stable at elevated pressures and

temperatures may be common phases in quartzofeldspathic granulites and need to be searched for.

Keywords: HIGH-TEMPERATURE STUDIES: kumdykolite, micro-Raman, micro-Raman mapping, BSE, WDX, high-temperature, ultrahigh-pressure, granulite, microdiamond

Introduction

Quartzofeldspathic diamond-bearing ultrahigh-pressure (UHP) granulites of the north Bohemian crystalline basement, European Variscan Belt (Kotková et al. 2011a, b) are favorable for the occurrence and preservation of rare K or Na feldspar modifications formed at extreme P-T conditions; this is due to their bulk rock composition (high ASI up to 1.5, high alkali content both reaching about 3 wt %) and rapid cooling during exhumation (Kotková et al. 1996; Zulauf et al. 2002). We report the presence of kumdykolite in one of the multiphase solid inclusions in garnet in felsic garnet-kyanite-feldspar-quartz granulite from the T7 borehole, located at the village of Staré in the České středohoří Mountains (see Kotková et al. 2011a, b). This orthorhombic form of $NaAlSi_3O_8$ was first described in diamondiferous eclogite from the UHP Kokchetav Massif, Kazakhstan as micrometer-sized inclusions in omphacite (Hwang et al. 2009), and recently from the Sahara 97072, 3H3 enstatite chondrite (Németh et al. 2013). Kumdykolite is metastable, and is presumed to be a high-temperature modification by analogy with the corresponding calcium end-member svyatoslavite (Hwang et al. 2009), although kumdykolite has not yet been synthesized. Svyatoslavite and dmisteinbergite (pseudo-orthorhombic and hexagonal $CaAl_2Si_2O_8$, respectively) are metastable phases at room temperature and pressure, crystallizing at temperatures as high as 1200–1400 °C. These two phases have been reported from burning coal dumps in

Chelyabinsk, Russia, and the latter recently discovered in the Allende meteorite (see Abe and Sunagawa 1995; Krivovichev et al. 2012; Ma et al. 2013).

The aim of this paper is to describe the mode of occurrence of kumdykolite and to discuss the possible use of its presence to the interpretation of P-T evolution of the rocks.

Experimental methods

Raman spectra were collected using a Thermo Scientific model DXR microscope equipped with a 532-nm line laser for excitation of mineral phases at the Institute of Chemical Technology Prague. Locations of interest were positioned using a motorized XY stage and an optical camera. The lateral resolution of the measurements was identical to the laser spot size, which was focussed by the 100x objective lens to about 1 μm. Analytical conditions were as follows: laser power about 10 mW, a spectrograph with holographic grating (400 gr. per mm) and pinhole width 25 μm, acquisition time 10 s, ten accumulations summed together to obtain a spectrum. A 1-μm step was selected for microspectroscopic line mapping using the OMNIC Atlμs imaging software program (ThermoFisher Scientific, Inc., MA, USA). The standard deviation of the wavenumber axis is 1.8 cm^{-1} with full-range grating.

Chemical analysis (WDX - wavelength dispersive X-ray spectroscopy) was performed on a CAMECA SX100 electron microprobe at the Department of Geological Sciences, Masaryk University using an accelerating voltage of 15 kV, beam current of 8 nA, and 4-μm beam diameter. The following standards were used: sanidine (K, Al, Si), wollastonite (Ca) and almandine (Fe). Back-scattered electron images (BSE) were captured at the same conditions. For standard deviation of the measurement see electronic supplement.[1] The mineral formula of kumdykolite was normalized on the basis of 5 cations.

Results

Kumdykolite has been identified in one of several multiphase solid inclusions (MSI) enclosed in a large (2.3 mm in diameter) garnet in a felsic, diamond-bearing, garnet-kyanite-feldspar-quartz granulite with late phlogopite (Kotková et al. 2011a, b; see electronic supplement[1] for a more detailed sample description). The MSI are near-isometric to elongated, reaching 20–50 μm in diameter, are characterized by curved boundaries and in the form of offshoots. They consist of phlogopite and quartz, some also contain phengitic mica, muscovite, amphibole, and graphite; accessory rutile, apatite, and pyrite are commonly present (Fig. 1).

BSE imaging coupled with micro-Raman mapping has shown that a subhedral, 20-μm long grain of kumdykolite is associated with phlogopite and quartz in one of the MSI (Figs. 1e and 2). Due to the large size of the kumdykolite grain, the Raman signal was strong and yielded good-quality Raman spectra characterized by vibration bands at 222, 464 and 492 cm^{-1}, with additional weak bands at 265 and 407 cm^{-1} (Fig. 3A). These bands correspond to the Raman spectra from Hwang et al. (2009), and differ from plagioclase feldspars, which have their characteristic, most intense bands between 500 and 510 cm^{-1} (Mernagh 1991; Freeman et al. 2008; Makreski et al. 2009; Fig. 3B). Absence of O-H-O bending Raman bands in the region of 3400–3700 cm^{-1} confirms the anhydrous character of the phase. Bands of quartz and garnet are also present (see Fig. 3A, 4). Overlap between the quartz and kumdykolite band at 464 cm^{-1} may cause the rather large change in the intensity of the band and its apparently high FWHM (full width at half maximum; Fig. 4). Nevertheless, the band at 155 cm^{-1} cannot be attributed to any of the associated phases, and it most probably represents another characteristic Raman band of kumdykolite not reported by Hwang et al. (2009). Whereas intense bands below about 300 cm^{-1} can be attributed to the lattice modes and stretching vibrations of Na-O bonds, the most intense bands in the spectrum of kumdykolite at 492 cm^{-1} and 462 cm^{-1} can be assigned to Si-O-Si or Si-O-Al bending (stretching) modes (Freeman et al. 2008; Makreski et al. 2009).

WDX analyses of kumdykolite revealed an elevated content of Ca (2.02 wt. % CaO; Table 1). As there is no Ca-rich mineral associated with kumdykolite in the MSI, and Mg content is not elevated, which precludes contamination from the host garnet that contains 5.6 wt. % CaO and 10.4 wt. % MgO, this presumably indicates significant solid solution with the Ca-endmember, svyatoslavite.

Phlogopite from the kumdykolite-bearing inclusion has a higher X_{Mg} (MgO/MgO+FeO = 0.76) and Al_2O_3 content (20.6 wt %) than those of the matrix phlogopite grains (0.60–0.65, 16–17 wt %, resp.). Its Si content (2.8 a.p.f.u.) is rather high, but similar to that of the matrix phlogopite. It contains less Ti than the phlogopite in the matrix (3.1–3.3 wt % TiO_2, 0.15 a.p.f.u. Ti). Phengitic mica in an inclusion, consisting of subhedral phlogopite with a small apatite inclusion and a large pyrite grain, contains 3.3 a.p.f.u. Si and 0.42 wt % TiO_2, whereas phengitic mica associated with Qtz (Fig. 1f) contains 3.14–3.16 a.p.f.u. Si, 0.15 wt % TiO_2 and 0.23–0.26 mol. % of paragonite component.

The kumdykolite-bearing inclusion is located close to the edge of the garnet core zone, characterized by high Ca and Mg contents. From EMP measurements, we determined the garnet composition next to the kumdykolite-bearing inclusion as $Prp_{40}Alm_{44}Grs_{12}Sps_1$.

Discussion

Kumdykolite composition and formation conditions

The CaO content of the kumdykolite (2.02 wt %) is much higher than the contents reported so far from the two other occurrences (≤ 0.49 wt. %: Hwang et al. 2009; Németh et al. 2013). Despite differences in proposed space groups, we believe that kumdykolite (orthorhombic, a = 8.24, b = 8.68, c = 4.84 Å) is more likely to form a solid solution with the Ca-endmember svyatoslavite (monoclinic, pseudo-orthorhombic, a = 8.23, b = 8.60, c = 4.85 Å) than with dmisteinbergite (hexagonal; Krivovichev et al. 2012). We therefore conclude that our

observations are the first indications of significant miscibility of kumdykolite with svyatoslavite (10 mol. % of svyatoslavite). Within a single thin section, another garnet of identical composition and zoning contains diamond within the same compositional zone. This provides evidence for entrapment of the kumdykolite-bearing inclusion at ultra-high pressure in the stability field of diamond. It was proposed that kumdykolite, similarly to svyatoslavite, can crystallize at temperatures as high as 1300 °C (Krivovichev et al. 2012; Németh et al. 2013). The character and mineral assemblages of the MSI may indicate if they crystallized at ultra-high temperature (Németh et al. 2013), close to the maximum burial of the rocks, or at lower temperatures during exhumation (Hwang et al. 2009).

Crystallization of the inclusion mineral assemblage and possible formation conditions of kumdykolite

MSI in the garnet studied contain mineral assemblages dominated by euhedral–subhedral phlogopite and quartz, with rarer phengitic mica or hornblende, and accessory rutile, apatite and pyrite. The rather uniform mineral assemblage, independent of the position within the garnet grain, precludes the possibility that these represent minerals or assemblages enclosed in garnet on the prograde path. Indeed, the offshoots filled with the inclusion minerals, along with the multiphase character of the inclusions and distinct mineral assemblages, suggest that these MSI may represent decrepitated fluid or melt inclusions. Fluid cannot be distinguished from melt at UHP conditions as the system is in the supercritical state. The offshoots result from the healing of fractures in the garnet host after the inclusion has been trapped, and occur because of their high internal overpressure (see Stöckhert et al. 2001; Bodnar 2003 for more details). We emphasize that graphite commonly occurs in MSI associated with quartz, whereas neither diamond nor coesite have been observed within these MSI.

The exhumation path of the studied granulites from the peak P-T conditions of > 4 GPa and about 1000 °C was dominated by near-to-isothermal decompression (Kotková et al. 1996, 2011a).

Large inclusions decrepitate more easily than small ones do, and at a lower differential pressure (i.e. internal pressure/confining pressure) when the rock follows an isothermal decompression path (i.e. is located in the "overpressure" P-T field; Bodnar et al. 2003; Stöckhert et al. 2009 and references therein). The presence of the lower-pressure polymorph of carbon, graphite, in large MSI with abundant textural evidence for re-equilibration by decrepitation in our sample therefore suggests that decrepitation occurred at high temperatures and at a relatively early time during rock exhumation.

Nucleation and growth of crystals in the inclusions, though, is likely to occur after decrepitation, one argument being that a drop in pressure is required for a drop in solubility (see e.g. Stöckhert et al. 2009). Our micro-Raman study has not revealed the presence of coesite (quartz is the only silica observed) that would indicate UHP conditions in the MSI. However, coesite has been described in the associated rocks (Kotková et. al. 2011a, b). The phengitic mica composition corresponds to P < 2.5 GPa, and temperatures as low as 650 °C, on the basis of the experimental data of Hermann and Spandler (2008). Low Ti content and high X_{Mg} of phlogopite in the inclusion also suggest rather low temperatures: the garnet-biotite thermometer of Bhattacharya et al. (1992) yields T < 600 °C for P < 2.5 GPa, which may, however, also be due to biotite re-equilibration due to Fe-Mg exchange with the surrounding garnet upon cooling.

We conclude that kumdykolite crystallized after the UHP and during the rapid cooling of the exhuming rocks. This agrees with the interpretation of Hwang et al. (2009) and the larger molar volume of kumdykolite (Németh et al. 2013) than those of the higher-pressure polymorphs of $NaAlSi_3O_8$, such as lingunite. The most important finding is that the

metastable phase kumdykolite is preserved, rather than forming albite at lower temperatures; this requires rapid cooling. Experimental work shows that the Ca-endmember, svyatoslavite, similar to other metastable phases, crystallizes earlier than the more-ordered anorthite in supercooled silicate melts (Abe et al. 1991; Abe and Sunagawa 1995; Krivovichev et al. 2012). Our study therefore represents another supportive argument for the possible presence of silicate melts in UHP rocks. More experimental studies of kumdykolite stability are needed before it can become a quantitative measure for the interpretation of the P-T evolution of rocks.

Implications

Apart from extending the database and list of occurrences of kumdykolite, our results should stimulate new studies of felsic, quartzofeldspathic granulites, which are very common in the European Variscan belt and elsewhere. Kumdykolite, and other feldspar modifications stable at elevated temperatures and pressures, can hardly be distinguished from plagioclase, or K-feldspar, by optical microscopy or EMP. It is therefore probable that the occurrence of these phases, which provide important constraints on the peak P-T conditions and evolution of rocks, may be common in similar rock types and need to be searched for. Micro-Raman spectroscopy represents a unique method for identification of such small-sized phases.

Acknowledgements

The financial support of the Czech Science Foundation project 13-21450S allowed for the acquisition of the analytical data and the writing of the paper. Constructive comments of J. Ague, S. Ferrero, P. Németh, an anonymous reviewer, and Ian Swainson, are gratefully acknowledged. J. Kotková also appreciates earlier discussions with P.J.O´Brien and Maria Perraki as a motivation and encouragement for this study.

199

200 **References cited**

201 Abe, T., and Sunagawa, I. (1995) Hexagonal $CaAl_2Si_2O_8$ in a high temperature solution:
202 metastable crystallization and transformation of anorthite. Mineralogical Journal, 17,
203 257-281.
204 Abe, T, Tsukamoto, K., and Sunagawa, I. (1991) Nucleation, growth and stability of
205 $CaAl_2Si_2O_8$ polymorphs. Physics and Chemistry of Minerals, 17, 473-484.
206 Bhattacharya, A., Mohanty, L., Maji. A., Sen, S.K., and Raith, M. (1992) Non-ideal mixing in
207 the phlogopite-annite binary: constraints from experimental data on Mg-Fe
208 partitioning and a reformulation of the biotite-garnet geothermometer. Contributions to
209 Mineralogy and Petrology, 111, 87-93.
210 Bodnar, R.J. (2003) Reequilibration of fluid inclusions. In I. Samson, A. Anderson and D.
211 Marshall, Eds., Fluid Inclusions: Analysis and Interpretation, p. 231-230. Mineralogical
212 Association of Canada, Short Course 32.
213 Freeman, J.J., Wang, A., Kuebler, K.E., Jolliff, B., and Haskin, L.A. (2008) Characterization
214 of natural feldspars by Raman spectroscopy for future planetary exploration. The
215 Canadian Mineralogist, 46, 1477-1500.
216 Herman, J., and Spandler, C.J. (2008) Sediment melts at sub-arc depths: an experimental
217 study. Journal of Petrology, 49, 717-740.
218 Hwang, S.-L., Shen, P., Chu, H.-T., Yui, T.-F., Liou, J.-G., and Sobolev, N.V. (2009)
219 Kumdykolite, an orthorhombic polymorph of albite, from the Kokchetav ultrahigh-
220 pressure massif, Kazakhstan. European Journal of Mineralogy, 21, 1325-1334.
221 Kotková, J., Kröner, A., Todt, W., and Fiala, J. (1996) Lower Carboniferous high-pressure
222 event in the Bohemian Massif: evidence from North Bohemian granulites.
223 Geologische Rundschau, 85, 154-161.

Kotková, J., O´Brien, P.J., and Ziemann, M.A. (2011a) Diamond and coesite discovered in Saxony-type granulite: solution to the Variscan garnet peridotite enigma. Geology, 39, 667-670.

—— (2011b) Diamonds in the Bohemian Massif – evidence for ultrahigh-pressure metamorphism. Geologické výzkumy na Moravě a ve Slezsku 18, 1, 35-38.

Krivovichev, S., Shcherbakova, E.P., and Nishanbaev, T.P. (2012) The crystal structure of svyatoslavite and evolution of complexity during crystallization of a $CaAl_2Si_2O_8$ melt: a structural automata description. The Canadian Mineralogist, 50, 585-592.

Ma, C., Krot, A.N., and Bizzarro, M. (2013) Discovery of dmisteinbergite (hexagonal $CaAl_2Si_2O_8$) in the Allende Meteorite: A new member of refractory silicates formed in the solar nebula. American Mineralogist, 98, 1368-1371.

Makreski, P., Jovanovski, G., and Kaitner, B. (2009) Minerals from Macedonia. XXIV. Spectra-structure characterization of tectosilicates. Journal of Molecular Structure, 924-926, 413-419.

Mernagh, T.P. (1991) Use of the laser Raman microprobe for discrimination amongst feldspar minerals. Journal of Raman Spectroscopy, 22, 453-457.

Németh, P., Lehner, S.W., Petaev, M.I., and Buseck, P. (2013) Kumdykolite, a high-temperature feldspar from an enstatite chondrite. American Mineralogist 98, 1070-1073.

Stöckhert, B., Duyster, J., Trepmann, C., and Massonne, H.J. (2001) Microdiamond daughter crystals precipitated from supercritical COH + silicate fluids included in garnet, Erzgebirge, Germany. Geology, 29, 391–394.

Stöckhert, B., Trepmann, C., and Massonne, H.J. (2009) Decrepitated UHP fluid inclusions: about diverse phase assemblages and extreme decompression rates (Erzgebirge, Germany). Journal of Metamorphic Geology, 27, 673-684.

Zulauf, G., Dörr, W., Fiala, J., Kotková, J., Maluski, H., and Valverde-Vaquero, P. (2002): Evidence for high-temperature diffusional creep preserved by rapid cooling of lower crust (North Bohemian shear zone, Czech Republic). Terra Nova, 14, 343-354.

Figure captions

Figure 1. BSE images of multiphase solid inclusions within garnet (2.3 mm in diameter) in felsic garnet-kyanite-feldspar-quartz granulite showing rather uniform assemblages of phlogopite and quartz, with less abundant phengitic mica and hornblende and accessory rutile, apatite and pyrite. e – kumdykolite-bearing inclusion.

Figure 2. Raman maps of the kumdykolite-bearing inclusion produced by color-coding the characteristic bands of individual minerals, with the intensity increasing from blue to red: a – kumdykolite (492 cm^{-1}), b - quartz (467 cm^{-1}), c – phlogopite (670 cm^{-1}).

Figure 3. A: Raman spectrum of kumdykolite. Additional bands correspond to the host garnet (Grt) and the associated phases quartz (Qtz) and phlogopite (Phl). B: Raman spectrum of albite (RRUFF database).

Figure 4. Raman spectra from the mapping segment with 1-μm step along the X axis, showing change in intensity of the 460/465 cm^{-1} band depending on the content of Qtz in the measured spot.

[1]Deposit item AM-XX-XXX, electronic supplement. Deposit items are available two ways: For a paper copy contact the Business Office of the Mineralogical Society of America (see inside front cover of recent issue) for price information. For an electronic copy visit the MSA web site at http://www.minsocam.org, go to the American Mineralogist Contents, find the table of contents for the specific volume/issue wanted, and then click on the deposit link there.

275
276

Table 1. Kumdykolite analysis

SiO_2	67.32
Al_2O_3	21.26
FeO	0.70
CaO	2.02
Na_2O	9.85
K_2O	0.04
Total	101.19
Si	2.946
Al	1.096
Fe	0.026
Ca	0.095
Na	0.835
K	0.002
An	0.10
Ab	0.90
Or	0.00

Figure 1

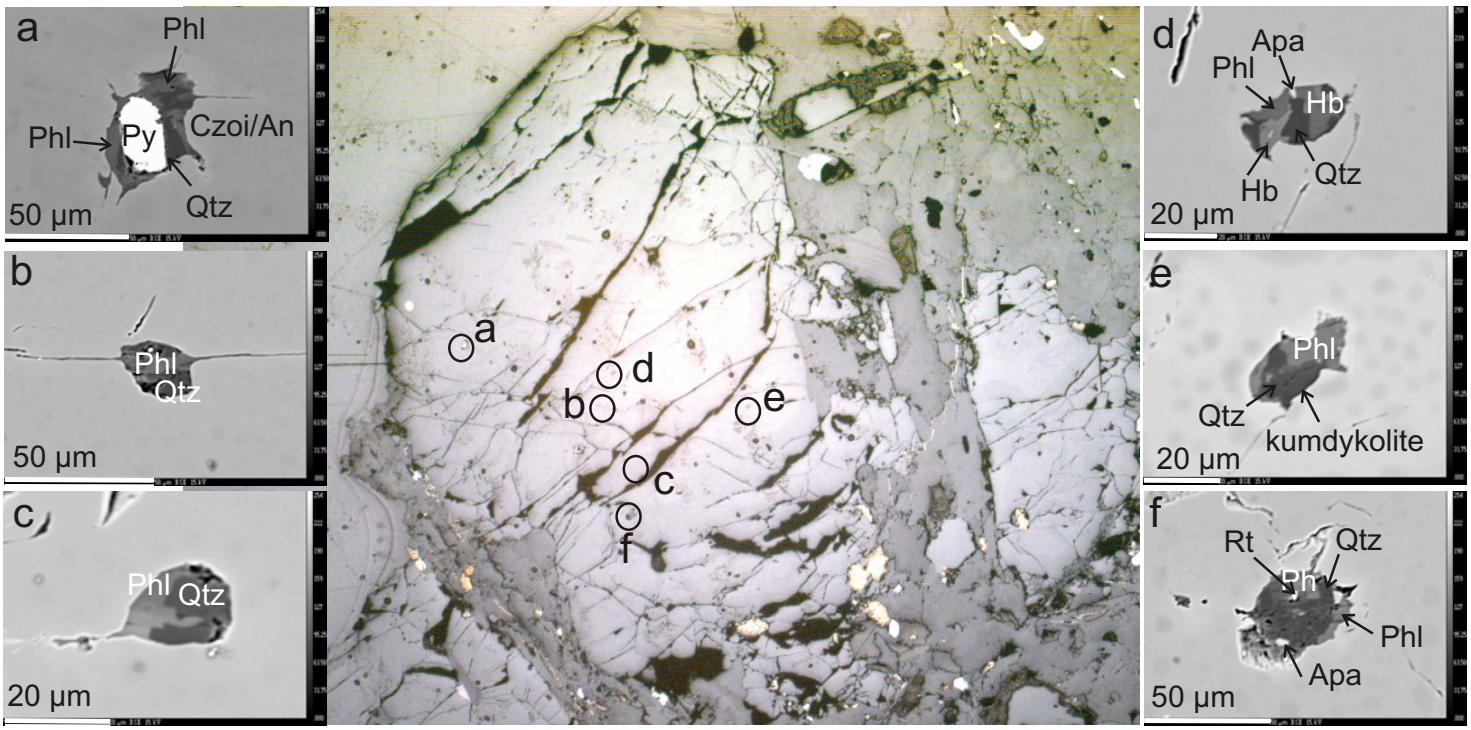
a
Phl
Phl
Py
Czoi/An
Qtz
50 µm
b
Phl
Qtz
50 µm
c
Phl
Qtz
20 µm
a
b
d
e
c
f
d
Apa
Phl
Hb
Hb
Qtz
20 µm
e
Phl
Qtz
kumdykolite
20 µm
f
Rt
Qtz
Ph
Phl
Apa
50 µm

This is a preprint, the final version is subject to change, of the American Mineralogist (MSA)
Cite as Authors (Year) Title. American Mineralogist, in press.
(DOI will not work until issue is live.) DOI: http://dx.doi.org/10.2138/am.2014.4889

Figure 2

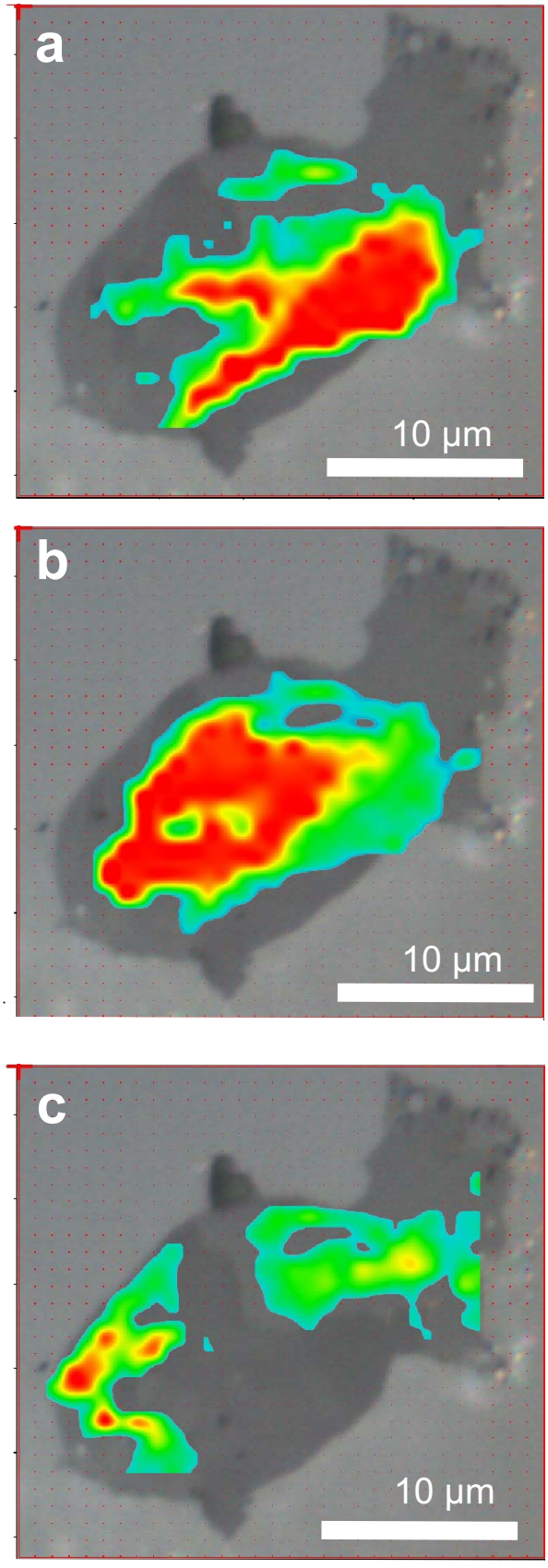

Figure 3

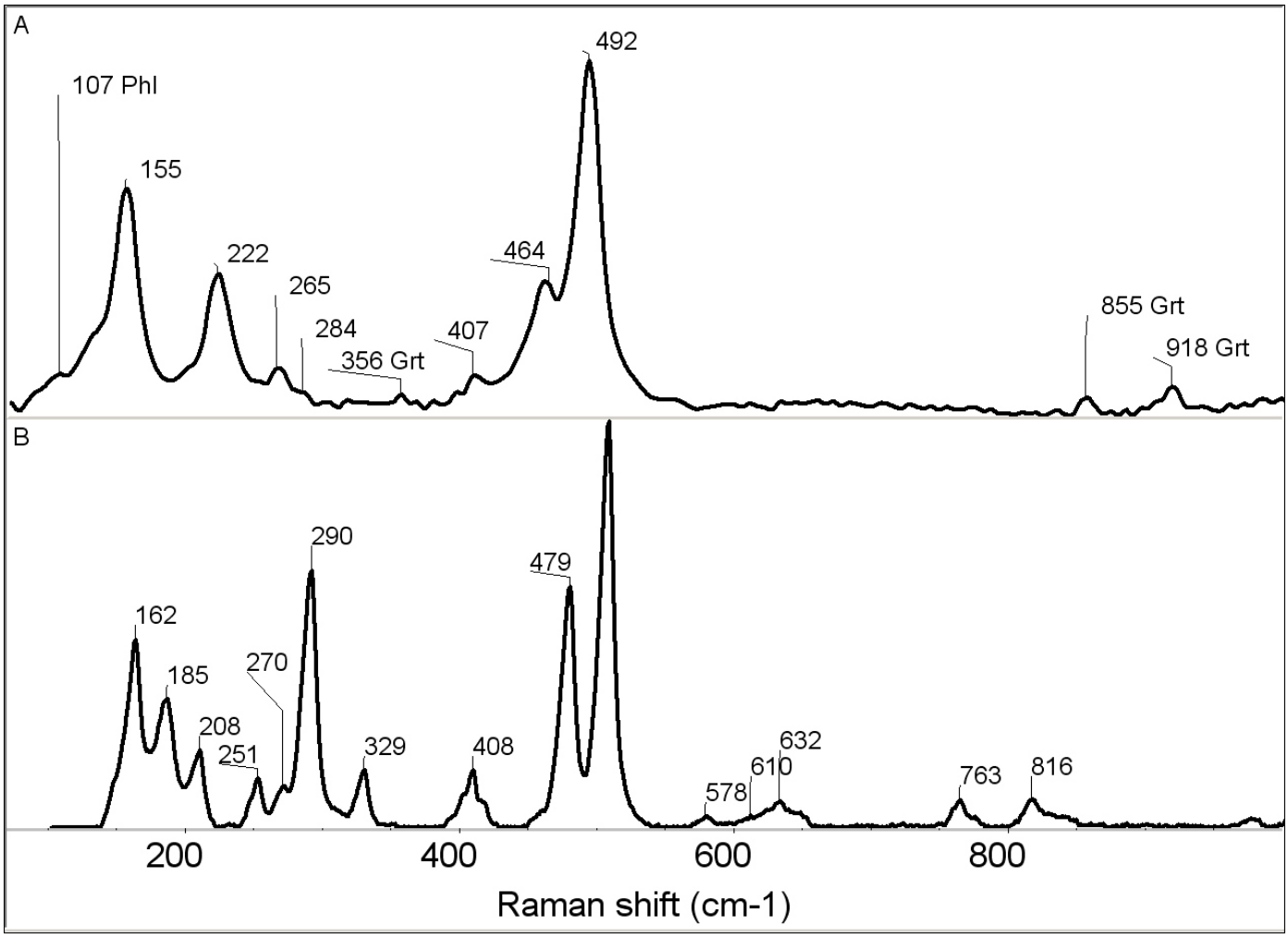
A
107 PhI
155
222
265
284
356 Grt
407
464
492
855 Grt
918 Grt
B
162
185
208
251
270
290
329
408
479
578
610
632
763
816
200
400
600
800
Raman shift (cm-1)

Figure 4

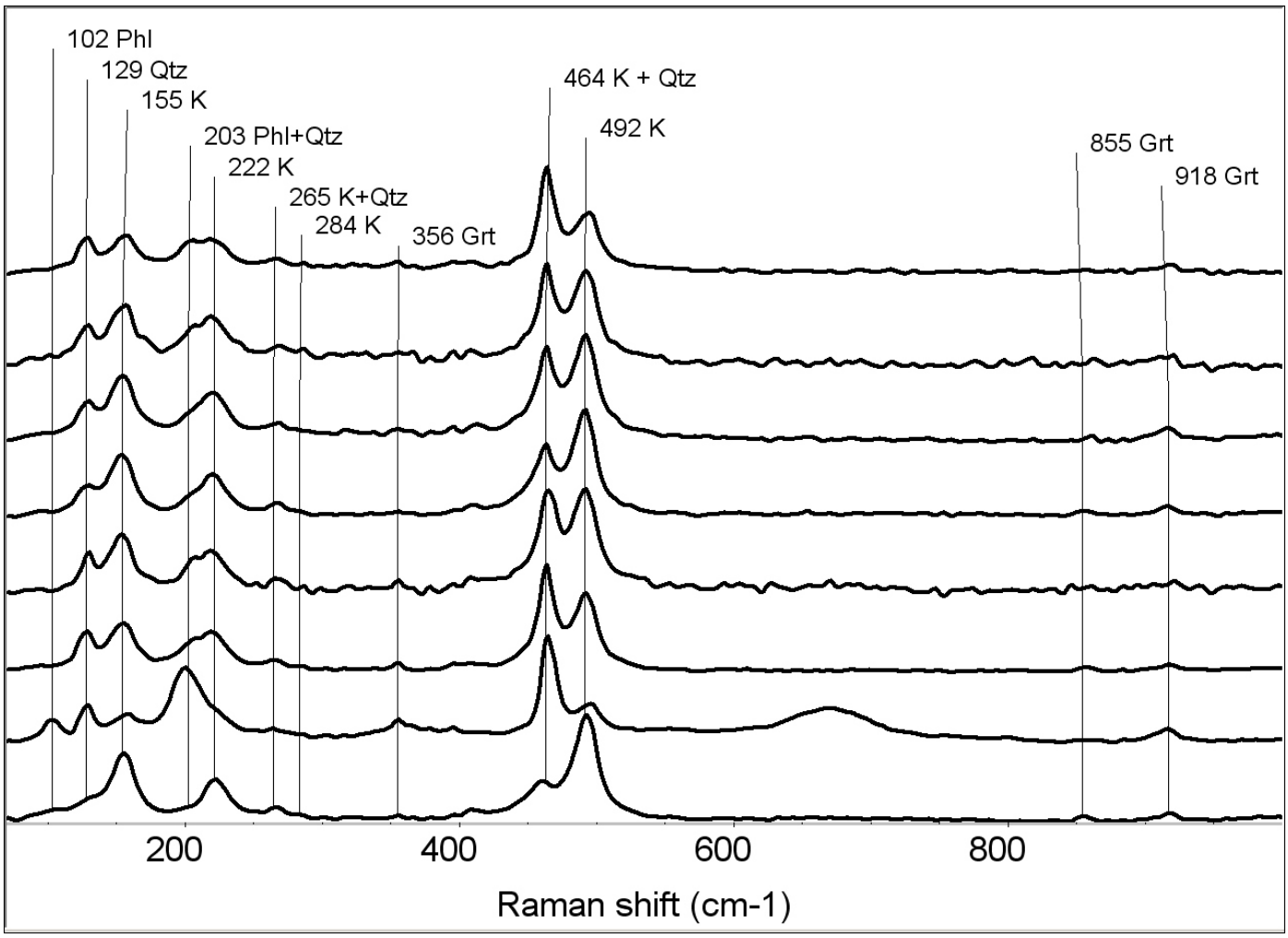
102 Phl
129 Qtz
155 K
203 Phl+Qtz
222 K
265 K+Qtz
284 K
356 Grt
464 K + Qtz
492 K
855 Grt
918 Grt
200
400
600
800
Raman shift (cm-1)